



Cross-linking of glycosphingolipids at the plasma membrane: consequences for intracellular signaling and traffic

Tove Irene Klokk^{1,2} · Simona Kavaliauskiene^{1,2,3} · Kirsten Sandvig^{1,2,3}

Received: 28 April 2015 / Revised: 16 September 2015 / Accepted: 17 September 2015 / Published online: 25 September 2015
© Springer Basel 2015

Abstract Glycosphingolipids (GSLs) are predominantly found in the outer leaflet of the plasma membrane, where they play a role in important processes such as cell adhesion, migration and signaling. However, by which mechanisms GSLs regulate these processes remains elusive. In this study, we therefore took advantage of the fact that some GSLs also serve as receptors for certain protein toxins, which rely on receptor binding for internalization and intoxication. Here, we demonstrate that Shiga and cholera toxins, which both possess multivalent GSL-binding capacity, induce dissociation of the cytosolic cPLA₂α–AnxA1 complex in HeLa and HMEC-1 cells. The dissociation is mediated through an increase in cytosolic calcium levels and activation of the tyrosine kinase Syk. Ricin, a protein toxin that does not cross-link surface molecules, has no effect on the same complex. Importantly, we find that antibody-mediated cross-linking of Gb3 and GM1, the GSL receptors for Shiga and cholera toxin, respectively, also induces dissociation. These data demonstrate that cross-linking of GSLs at the plasma membrane mediates the intracellular signaling events

resulting in dissociation of the complex. After dissociation, cPLA₂α and AnxA1 are translocated to intracellular membranes where they are known to function in regulating membrane transport processes. In conclusion, we have characterized a novel mechanism for cell surface-induced initiation of intracellular signaling and transport events.

Keywords Glycosphingolipids · Cross-linking · Calcium · Syk · Annexin · Phospholipase A2

Introduction

Cellular membranes of eukaryotes are made up of phospholipids, sphingolipids and sterols, and are dynamic organelles that respond to extracellular and intracellular stimuli [1]. Glycosphingolipids (GSLs) are sphingolipids with an oligosaccharide attached to its ceramide backbone. GSLs are predominantly found in the outer leaflet of the plasma membrane, where the hydrophobic backbone serves as a membrane anchor and the hydrophilic oligosaccharide chain is exposed on the cell surface (for review, see [2]). GSLs are often found in lipid microdomains termed lipid rafts, domains enriched in cholesterol and sphingolipids. The nature and dynamics of these domains are under investigation [3] and they have been proposed to act as platforms in the membrane, mediating transfer of signals from extracellular ligands via lipids, transmembrane proteins and intracellular signaling molecules [4]. GSLs are also critical for cell adhesion, migration and differentiation [5, 6]; however, the molecular details of these processes are far from understood. Importantly, changes in GSL composition and metabolism are associated with oncogenic transformation, and different GSLs are overexpressed in several cancer types [7, 8]. Elucidating how ligand binding

Electronic supplementary material The online version of this article (doi:10.1007/s00018-015-2049-1) contains supplementary material, which is available to authorized users.

✉ Tove Irene Klokk
toklok@rr-research.no

¹ Department of Molecular Cell Biology, Institute for Cancer Research, The Norwegian Radium Hospital, Oslo University Hospital, 0379 Oslo, Norway

² Centre for Cancer Biomedicine, Faculty of Medicine, University of Oslo, 0316 Oslo, Norway

³ Department of Biosciences, University of Oslo, 0316 Oslo, Norway

to GSLs may induce intracellular signaling and transport events is therefore crucial to better understand how over-expression of GSLs may be involved in cancer development and progression.

GSLs serve as receptors for toxins, bacteria, viruses and fungi, and are involved in pathogen-induced signaling [9]. Shiga toxin (Stx), a protein toxin produced by the bacteria *Shigella dysenteriae* and certain *E. coli* strains, requires binding to its GSL receptor Gb3 (globotriaosylceramide) for successful intoxication. Stx is internalized by endocytosis after binding to the oligosaccharide part of Gb3 and is transported retrogradely through the Golgi apparatus and the endoplasmic reticulum to its final destination, the cytosol, where it inhibits protein synthesis (for recent reviews on Shiga toxin, see [10, 11]). We have previously shown that Stx is able to induce dissociation of the cytosolic complex of annexin A1 (AnxA1) and the phospholipase A2, cPLA₂α [12]. The function of annexins is linked to their ability to bind membrane phospholipids in a dynamic and reversible fashion through their Ca²⁺-binding domains, providing a connection between Ca²⁺ signaling and membrane functions [13]. Studies from our laboratory have shown that AnxA1 plays a role in the retrograde transport of Stx, where depletion of AnxA1 results in increased transport of Stx to the Golgi, an effect that is dependent on cPLA₂α activity [12]. Phospholipase A2 (PLA₂) is a class of enzymes that removes a fatty acid from phospholipids at the *sn*-2 position, converting cone- or cylindrical-shaped phospholipids to inverted cone-shaped lysophospholipids [14]. cPLA₂α, a Ca²⁺-dependent cytosolic PLA₂, has been specifically implicated in intra-Golgi transport [15] and has been reported to associate with the Golgi complex upon increases in cytosolic Ca²⁺ concentration [16–18]. Both these proteins are thus implicated in membrane function and membrane transport processes.

To better understand how ligand binding to GSL receptors at the cell surface might mediate intracellular signaling and trafficking events, we first set out to elucidate by which mechanisms Stx induces dissociation of the cPLA₂α–AnxA1 complex. We then tested whether these mechanisms are general for cross-linking of GSLs by applying cholera toxin (Ctx) and also antibodies causing cross-linking of Gb3 and GM1, the GSL receptors for Stx and Ctx, respectively. The data presented clearly show that GSL cross-linking at the plasma membrane induces an increase in intracellular calcium and activation of the tyrosine kinase Syk, eventually leading to dissociation of the cPLA₂α–AnxA1 complex, followed by translocation of the complex components to intracellular membranes. Our data thus provide novel information on how protein–lipid interactions at the plasma membrane initiate signaling events with consequences for intracellular transport.

Materials and methods

Reagents and antibodies

All chemicals were purchased from Sigma-Aldrich (St. Louis, MO, USA) unless stated otherwise. The AnxA1, cPLA₂α, Hsp90 and flotillin-2 antibodies used for immunoblot analysis, and the IgM Gb3 and control IgM antibodies used in the proximity ligation assay (PLA), were from BD Biosciences (NJ, USA). The IgG GM1 antibody and the GAPDH antibody were from Abcam (Cambridge, MA, USA), and the pSyk (Y319) and totSyk antibodies were from Cell Signaling (Boston, MA, USA). The rabbit cPLA₂α antibody used for the PLA assay was from Santa Cruz Biotechnology (CA, USA), and the rabbit LAMP1 antibody used for immunofluorescence was from Sigma-Aldrich (St. Louis, MO, USA). The HRP-, Cy2- and Cy3-conjugated secondary antibodies were from Jackson ImmunoResearch (PA, USA). The plasmid expressing ShigaB-sulf2 (StxB-S2) was a gift from Dr. B. Goud (Institut Curie, Paris, France) and StxB-S2 was prepared as described elsewhere [19]. Shiga-like toxin 1 mutant (SLT1) was produced as described in [20], and ricin with a modified ricin A-subunit containing a tyrosine sulfation site was produced and purified as described earlier [21]. Cholera toxin (Ctx) was purchased from Sigma-Aldrich (St. Louis, MO, USA), and human recombinant galectin-3 was purchased from R&D Systems (Minneapolis, MN, USA). Plasmid for expression of wild-type Syk was prepared as described in [19].

Inhibitors

Inhibitors were purchased from Sigma-Aldrich (St. Louis, MO, USA) unless otherwise stated and used at the following concentrations: 10 mM methyl-β-cyclodextrin, 2 μM A23187, 10 μM piceatannol, 10 μM BAPTA-AM, 10 μM Syk Inhibitor V (Millipore, Billerica, MA, USA), 2.5 μM R406, 1.5 μM thapsigargin and 250 μM verapamil.

Cell culture

HeLa and HMEC-1 cells were maintained in Dulbecco's modified Eagle's medium (Invitrogen, Carlsbad, CA, USA) supplemented with 10 % fetal calf serum, 100 units/ml penicillin and 100 μg/ml streptomycin at 37 °C and 5 % CO₂. For the proximity ligation assay (PLA) and immunofluorescence experiments, the cells were seeded in six-well plates with two coverslips per well at a density of 2 × 10⁵ cells/well 1 day prior to experiment. For transfection, HeLa cells were seeded in six-well plates at a density of 1 × 10⁵ cells/well in growth medium without

antibiotics 1 day before transfection. For the calcium release assay, HeLa cells were seeded in 96-well plates (black with glass bottom) at a density of 1×10^4 cells/well 1 day before the experiment. For co-immunoprecipitation and fractionation experiments, HeLa cells were seeded in 10 cm plates at a density of 1×10^6 cells/plate 1 day before the experiment. For verification of the efficiency of the Syk siRNA oligoes, HeLa cells stably expressing GFP-tagged human Syk were used. The stable cell line was a lentivirus-generated pool using Gateway LR reactions (Invitrogen) and was maintained as described for HeLa and HMEC-1 cells.

Proximity ligation assay (PLA)

HeLa or HMEC-1 cells were incubated in Hepes-buffered medium for 2 h, followed by pre-incubation with inhibitors at indicated concentrations for 30 min before addition of 1 $\mu\text{g/ml}$ StxB-S2, Ctx or ricin, 1.5 $\mu\text{g/ml}$ SLT1, 20 $\mu\text{g/ml}$ Gb3 or IgM antibodies for 10 min at 37 °C, or 3 $\mu\text{g/ml}$ GM1 antibody alone or in the presence of anti-rabbit secondary antibody for 30 min at 37 °C. Galectin-3 was used at 1 or 2 $\mu\text{g/ml}$ for 30 min at 37 °C. When specified, the assay was performed in Hanks' balanced salt solution without calcium (Gibco, Carlsbad, CA 92008 USA). The proximity between AnxA1 and cPLA₂ α was evaluated using the PLA kit, DuolinkTM (Olink Bioscience, Uppsala, Sweden), according to the manufacturer's instructions. Briefly, after fixation in 10 % formalin solution and permeabilization with 0.1 % Triton X-100, primary antibodies against AnxA1 and cPLA₂ α were used either alone as negative controls, or in combination. Cells were then incubated with PLUS and MINUS secondary PLA probes conjugated with oligonucleotides against both rabbit and mouse IgG. The two complementary oligonucleotides were then hybridized, ligated and amplified by the provided polymerase, resulting in red fluorescence signals when the targeted proteins were closer than 40 nm. The cells were imaged at a Zeiss LSM780 laser scanning microscope (Carl Zeiss, Jena, Germany) equipped with a 60 \times objective, NA 1.4, using an open pinhole. The number of fluorescence spots per cell was quantified using ImageJ software (NIH, Bethesda, USA), and the average number of spots per cell was calculated. Typically, 35–40 cells were analyzed per condition in each experiment.

Co-immunoprecipitation (co-IP)

HeLa cells were starved in Hepes-buffered medium for 2 h before treatment with 1 $\mu\text{g/ml}$ StxB-S2 or 1.5 $\mu\text{g/ml}$ SLT1 for 30 min at 37 °C. The cells were then washed in cold PBS and lysed in lysis buffer (0.1 M NaCl, 10 mM Na₂HPO₄, 1 mM EDTA, 1 % Triton X-100, 60 mM octyl- β -

glycopyranoside, pH 7.4) supplemented with Complete protease inhibitors and PhosSTOP (Roche Diagnostics, Mannheim, Germany) on ice. The lysate was cleared by centrifugation at 4 °C (14,000 rpm, 20 min). Protein G-Sepharose beads (Amersham Biosciences, Buckinghamshire, UK) in PBS were incubated with anti-cPLA₂ α antibody for 2 h before washing with PBS. Beads pre-bound to antibody were mixed with the lysates and incubated at 4 °C overnight. After extensive washing, associated proteins were eluted by boiling at 100 °C for 5 min, separated by SDS-PAGE and blotted onto a PVDF membrane (Immobilon-P, Millipore, Billerica, MA, USA). The membrane was processed and the bands detected and quantified as described for immunoblot analysis.

Transfection

For analysis of Syk phosphorylation, HeLa cells were transfected with 0.25 $\mu\text{g/well}$ of a plasmid expressing wild-type Syk using FuGene 6 according to the manufacturer's recommendation (Roche Diagnostics, Mannheim, Germany). After 24 h, the cells were starved in Hepes-buffered medium for 2 h before treatment with 1 $\mu\text{g/ml}$ StxB-S2 or Ctx, or 1 μM H₂O₂ for the indicated time points at 37 °C. The cells were then lysed and subjected to immunoblot analysis. For depletion of Syk, cells were transfected with 50 nM Syk-specific siRNA oligos using RNAiMax according to the manufacturer's recommendations (Invitrogen, Paisley, UK). The following ON-TARGETplus siRNA oligoes were used: Syk#1 5'AGAAAUGUGUUGC UAGUUA-3', Syk#2: 5'-CGGAAUGCAUCAACUACUA-3' (Dharmacon, Lafayette, CO, USA). As a control, the cells were transfected with 50 nM of a non-targeting siRNA oligo (Dharmacon). Three days after transfection, the cells were subjected to PLA or immunoblot analysis.

Immunoblot

Treated cells were washed in PBS and lysed in lysis buffer [0.1 M NaCl, 10 mM Na₂HPO₄, 1 mM EDTA, 1 % Triton X-100, 60 mM octyl- β -glycopyranoside, pH 7.4] supplemented with Complete protease inhibitors and PhosSTOP (Roche Diagnostics, Mannheim, Germany) on ice. The lysate was cleared by centrifugation (14,000 rpm, 20 min) and separated by SDS-PAGE under reducing conditions. After blotting onto a PVDF membrane (Immobilon-P, Millipore, Billerica, MA, USA), the membrane was blocked in 5 % reconstituted skim milk (RSM) for 1 h at room temperature. Thereafter, the membrane was washed in PBS with 0.1 % Tween (PBS-T) or TBS with 0.1 % Tween (TBS-T) for pSyk immunoblot, and the primary antibody in 5 % BSA was applied overnight at 4 °C. After 3 \times 5 min washes in PBS-T (TBS-T) and incubation in

secondary antibodies and several washes in PBS-T (TBS-T), the bands were developed using the Supersignal West Dura kit from Thermo Scientific (Rockford, IL, USA). The bands were quantified using Image Lab software (BioRad Laboratories Inc, Hercules, CA, USA).

Calcium release assay

HeLa cells were incubated in Hepes-buffered medium for 2 h before treatment with the indicated inhibitors for 30 min at 37 °C. The change in intracellular calcium upon addition of 1 µg/ml StxB-S2, Ctx or ricin was measured using the Fluo-4 NW calcium Assay Kit from Molecular probes (Oregon, USA) according to the manufacturer's recommendations. When indicated, the assay was performed in calcium-free Hanks' balanced salt solution (Gibco, Carlsbad, CA 92008 USA) supplemented with 20 mM Hepes and 0.5 mM MgCl₂. In brief, Fluo-4 dye solution was added to the cells after removing the medium. If inhibitors were used, they were applied together with the dye. After 30 min incubation at 37 °C, the indicated ligand was automatically added using a syringe dispenser, and the fluorescence was measured every 10 or 20 s for 4 or 10 min on a Synergy2 plate reader (BioTek, VT, USA) using 485/20 and 528/20 excitation and emission filters, respectively. Three to four measurements were done before addition of toxin, and four replicate wells were measured at each time point. The results are presented as change in fluorescence over time relative to pre-injection fluorescence.

Cytosolic and membrane fractionation

HeLa cells were incubated in Hepes-buffered medium for 2 h before 1 µg/ml StxB-S2 or 2 µM A23187 was added. After 30 min incubation at 37 °C, the cells were washed twice in ice cold PBS, scraped in 1 ml PBS and the cell pellet spun down at 3000 rpm for 5 min. The cell pellet was dissolved in 100 µl homogenization buffer [0.25 M sucrose in 3 mM Imidazole containing Complete protease inhibitors and PhosSTOP (Roche Diagnostics, Mannheim, Germany)], using a 23 G syringe, without destroying the nuclei. After spinning at 6000 rpm for 5 min, the supernatant was transferred to an ultracentrifuge tube and centrifuged at 65,000 rpm for 15 min. The pellet (the membrane fraction) was dissolved in 40 µl homogenization buffer, and the supernatant was the cytosolic fraction. All of the membrane fraction and equal parts of the cytosolic fraction were separated by SDS-PAGE electrophoresis and subjected to immunoblot analysis. The membrane fraction of AnxA1 and cPLA₂α was calculated as % of control after normalization to the level of flotillin-2.

Confocal microscopy

HMEC-1 cells were incubated in Hepes-buffered medium for 2 h before treatment with StxB-S2 (1 µg/ml) for 30 min at 37 °C. The cells were washed twice in PBS and thereafter fixed with 10 % formalin solution for 15 min at room temperature, followed by permeabilization in 0.1 % Triton X-100 for 2 min at room temperature. The cells were incubated in blocking solution, 5 % fetal calf serum in PBS, for 30 min before incubation with the appropriate primary and secondary antibodies. The cells were mounted in Prolong[®]Gold containing DAPI for staining of the nuclei (Molecular Probes, Eugene, OR, USA) and imaged on a laser scanning confocal microscope LSM780 (Carl Zeiss, Jena, Germany), equipped with a 60× objective, NA 1.4. Images were prepared and analyzed with the ZEN software (Carl Zeiss, Jena, Germany) or ImageJ software (NIH, Bethesda, USA). Colocalization was quantified by calculating the Manders colocalization coefficient using the ZEN software (Carl Zeiss, Jena, Germany). Typically, 20–25 cells were analyzed per condition in each experiment.

Statistical analysis

Statistical analysis was performed using the two-tailed, paired Student's *t* test. A *p* value <0.05 was regarded as statistically significant.

Results

Shiga toxin-induced dissociation of the cPLA₂α–AnxA1 complex

Shiga toxin (Stx) consists of a pentameric B-subunit responsible for Gb3-binding, and an enzymatically active A-subunit [10]. We previously showed that a modified Stx B-subunit containing two sulfation sites (StxB-S2), induced dissociation of the cPLA₂α–AnxA1 complex [12]. To investigate whether the intact Stx, containing both A- and B-chains, would induce a similar dissociation of this complex, HeLa cells were incubated with equal molar concentrations of StxB-S2 or SLT1, an enzymatically inactive Stx mutant [20]. The complex dissociation was assayed by PLA where a fluorescence signal is produced when two molecules are within a distance of 40 nm. The data show that the number of signals per cell was reduced by approximately 60 % both by StxB-S2 and the intact toxin, indicating dissociation of the cPLA₂α–AnxA1 complex (Fig. 1a, b). A similar effect was also observed by using the PLA assay in the human microvascular endothelial cell line HMEC-1 (supplementary Fig. S1a), demonstrating that the dissociation is not restricted to HeLa

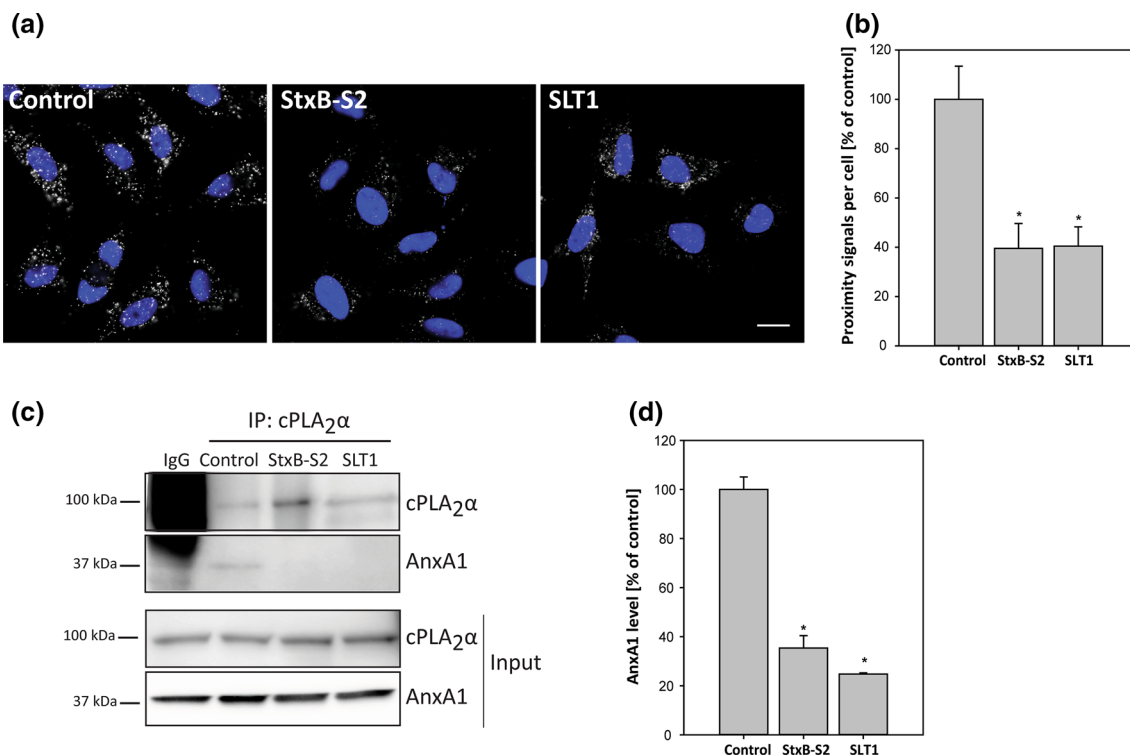


Fig. 1 Dissociation of cPLA₂α–AnxA1 induced by Shiga toxin. **a** HeLa cells were treated with 1 μg/ml ShigaB-sulf2 (StxB-S2) or 1.5 μg/ml Shiga-like toxin 1 mutant (SLT1) for 10 min before being fixed, permeabilized and subjected to PLA using cPLA₂α and AnxA1 antibodies. Representative images taken by a LSM780 confocal microscope are shown. Nucleus is stained by DAPI in blue, scale bar 20 μm. **b** Quantification of experiment as described in **a**, presented as % of control ($n = 5$ independent experiments, mean values +SEM, $*p < 0.05$). **c** HeLa cells were treated with 1 μg/ml StxB-S2 or

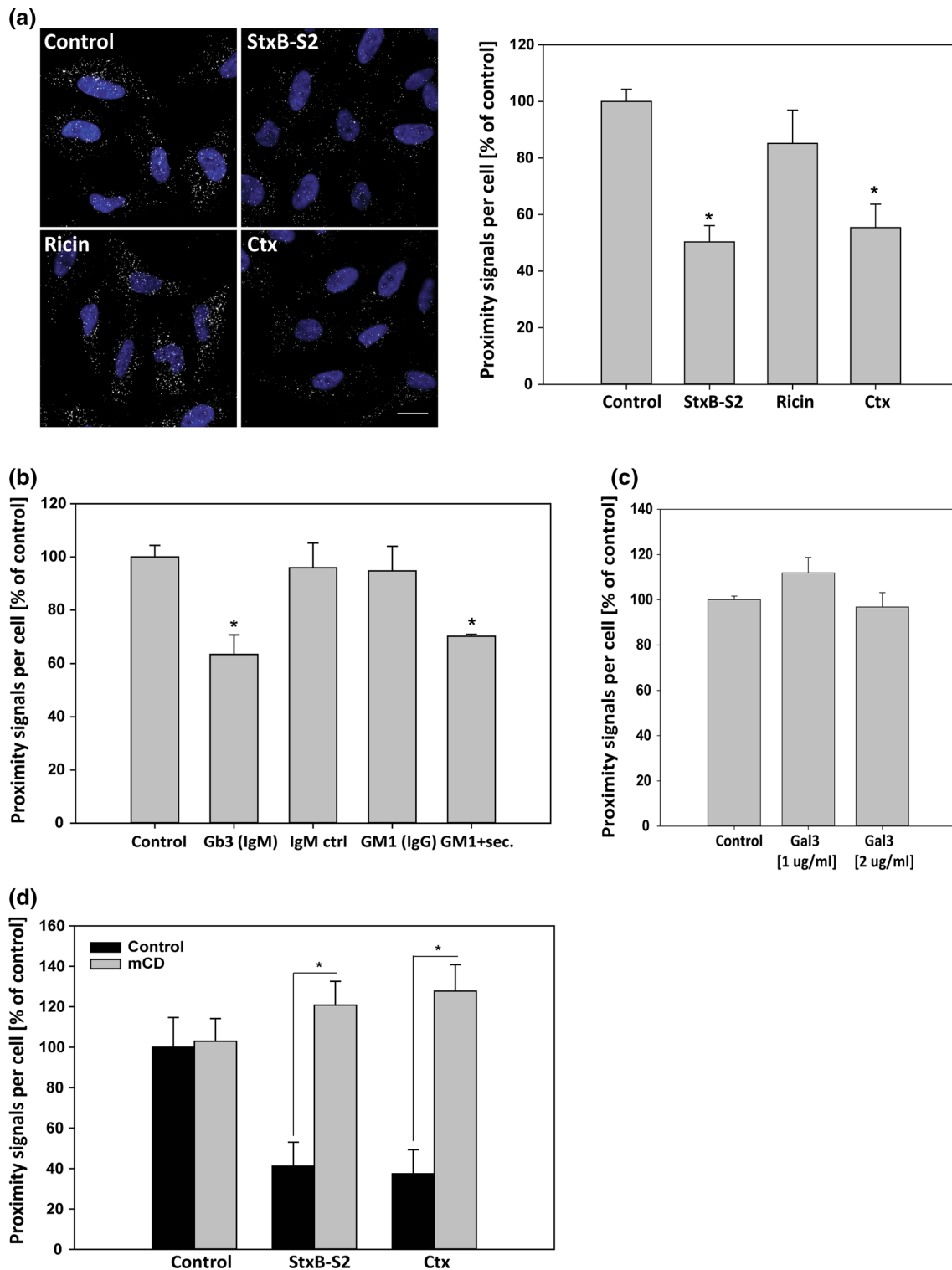
1.5 μg/ml SLT1 for 10 min and the cell lysates were subjected to immunoprecipitation with a cPLA₂α antibody, followed by immunoblot analysis using AnxA1 and cPLA₂α antibodies. Non-specific rabbit IgG antibody was used as negative control. The levels of AnxA1 and cPLA₂α in the input lysates are shown in the *two lower panels*. **d** Quantification of experiments as described in **c**, with AnxA1 levels normalized to cPLA₂α levels and presented as percentage of control ($n = 3$ independent experiments +SEM, $*p < 0.05$)

cells. Furthermore, co-IP of AnxA1 with cPLA₂α was strongly reduced after treatment with StxB-S2 or SLT1, confirming the ability of Stx to induce dissociation of the complex (Fig. 1c, d). A non-specific rabbit IgG antibody was used as a negative control for the co-IP, however it did not give a strong band at the size of cPLA₂α, probably due to the fact that a rabbit secondary antibody was used for detection of cPLA₂α. Importantly, the IgG did not give a band at the size of AnxA1. The specificity of the co-IP was further confirmed by the absence of bands following the treatment with StxB-S2 and SLT1.

Multivalent glycosphingolipid-binding is required for dissociation

In order to investigate if the observed dissociation of cPLA₂α–AnxA1 also might apply to other protein toxins, the PLA was performed with the plant toxin ricin and the bacterial protein toxin cholera toxin (Ctx), and the data show that Ctx, but not ricin, is able to induce dissociation of the complex (Fig. 2a). The binding subunit of Stx is a

homopentamer of 5 separate B-chains, each harboring three binding sites for Gb3 [22]. The binding of Stx to Gb3 thus involves multivalent protein-lipid binding, and leads to cross-linking of Gb3 molecules in the plasma membrane. Ricin on the other hand, does not cross-link surface molecules as it consists of an A-chain and a single peptide B-chain, responsible for binding to terminal galactose of lipids and proteins at the cell surface [23]. Similar to Stx, Ctx consists of five binding subunits, each with one binding site for its receptor the ganglioside GM1 (for a review on Ctx, see [24]). Ctx thus also cross-links GSLs at the cell surface, and importantly, Ctx also induces dissociation of the cPLA₂α–AnxA1 complex (Fig. 2a). These data therefore suggest that cross-linking of GSLs is required for the dissociation process. To investigate this further, we used an IgM anti-Gb3 antibody, which also binds Gb3 in a multivalent manner, and indeed, this antibody also induced dissociation, although to a somewhat lesser extent than the toxins (Fig. 2b). Dissociation induced by the Gb3 antibody was also observed in HMEC-1 cells (supplementary Fig. S1a). A non-targeting IgM antibody did not affect the



complex, neither did an IgG anti-GM1 antibody not possessing multivalent binding capacity. However, when the IgG anti-GM1 antibody was cross-linked by a secondary antibody (GM1 + sec), dissociation was induced (Fig. 2b). Together these data strongly support the idea that cross-

linking of GSLs in the plasma membrane is a requirement for the observed dissociation of the cytosolic cPLA₂ α -AnxA1 complex. The effect of StxB-S2 and Ctx on the complex is quite rapid, as a strong reduction in proximity signals is seen already after 5 min. However, the effect is

Fig. 2 Multivalent glycosphingolipid binding induces dissociation of cPLA₂α–AnxA1. **a** HeLa cells were treated with 1 μg/ml ShigaB-sulf2 (StxB-S2), ricin, or cholera toxin (Ctx) for 10 min before being fixed, permeabilized and subjected to PLA using cPLA₂α and AnxA1 antibodies. Representative images taken by an LSM780 confocal microscope are shown. The nucleus is stained by DAPI in blue; scale bar 20 μm. The bar graph shows the quantification of the number of signals per cell, presented as % of control. The mean values of at least three independent experiments are shown +SEM, **p* < 0.05. **b** HeLa cells were treated with 20 μg/ml IgM anti-Gb3 or control IgM antibodies for 10 min, or 3 μg/ml IgG anti-GM1 antibody alone or in combination with secondary antibody (sec) for 30 min, before being processed for the PLA as described in **a**. The mean values of at least three independent experiments are shown +SEM, **p* < 0.05. **c** The same experiment as in **a** and **b**, only after treatment with 1 or 2 μg/ml Gal3 for 30 min (*n* = 3 independent experiments +SEM). **d** HeLa cells were pre-treated with 10 mM methyl-β-cyclodextrin (mCD) for 30 min, followed by treatment with 1 μg/ml StxB-S2 or Ctx for 10 min, before being processed for the PLA assay as described in **a** (*n* = 4 independent experiments, mean values +SEM, **p* < 0.05)

stronger (and significant for both toxins) at 10 min (supplementary Fig. S1b). After 20 min, the effect has disappeared, at this time there is no longer significant differences from the control (supplementary Fig. S1b). This indicates that it is the initial binding of the toxins to their receptors that mediates the signaling events required for dissociation of the complex, and that the dissociation is reversible.

In order to elucidate if also cross-linking of glycoproteins would induce dissociation of the complex, we tested the effect of Galectin-3 (Gal3) in the PLA. Gal3 is a member of the galectin family of N-glycan binding proteins, however, Gal3 is unique in that it combines a carbohydrate recognition domain with a non-lectin domain that favors the formation of Gal3 oligomers including pentamers [25, 26], and thus cross-linking of glycoproteins at the plasma membrane. Furthermore, Gal3-oligomerizations is also suggested to promote GSL binding [27]. However, no dissociation of the cPLA₂α–AnxA1 complex was observed after treatment with either 1 or 2 μg/ml of Gal3 (Fig. 2c), although binding of Gal3 to HeLa cells was confirmed by flow cytometry (supplementary Fig. S1d).

As mentioned in the introduction, GSLs are often found in lipid rafts together with cholesterol [3]. The presence of lipid rafts seems to be a requirement for the ability of the toxins to induce dissociation, as extraction of cholesterol using methyl-β-cyclodextrin (mCD) inhibits the toxin-induced dissociation of the cPLA₂α–AnxA1 complex (Fig. 2d).

Complex dissociation involves Syk activation and an increase in intracellular calcium

Several kinases are activated upon Stx binding, such as the Src kinases Yes [28] and Lyn [29], the tyrosine kinase Syk [19], the MAPK p38α [30], and the serine/threonine kinase

PKCδ [31]. These phosphorylation events are implicated in clathrin-mediated endocytosis of Stx from the plasma membrane [19, 32, 33] and in transport to the Golgi apparatus [30, 31]. Based on these findings, we treated HeLa cells with inhibitors of signaling molecules known to be activated by Stx or implicated in Stx transport, in addition to compounds interfering with intracellular calcium levels, to investigate whether these are involved in the cPLA₂α–AnxA1 dissociation induced by Stx. Inhibitors of PKCδ, p38, Src, PKC, PI3K and CaMKII (calmodulin dependent kinase II) did not seem to interfere with the ability of StxB-S2 to induce dissociation of the complex (supplementary Fig. S1c). However, after pretreatment with the calcium chelator BAPTA-AM or the Syk inhibitor Piceatannol, StxB-S2 did not induce dissociation of the complex, suggesting that intracellular calcium and Syk activation is involved in the Stx-induced dissociation of cPLA₂α–AnxA1 (supplementary Fig. S1c). The calcium ionophore A23187 lowered the complex level by itself, and no further dissociation was induced by addition of StxB-S2 (supplementary Fig. S1c).

Syk is a non-receptor tyrosine kinase known to be involved in receptor internalization and traffic (see [34] for review). Previous work from our laboratory has shown that Stx induces Syk activation in HeLa cells, an activation that is inhibited by Piceatannol [19]. To investigate if Syk activation is induced by Ctx in a similar manner, phospho Syk-specific immunoblot was performed after treatment with the toxins for different time points. H₂O₂ was used as a positive control for Syk activation. The level of activated Syk (pSyk) was increased after 2.5, 5 and 10 min of treatment with StxB-S2 and after 5 and 10 min with Ctx, demonstrating that both toxins activate Syk (Fig. 3a, b). Only the timepoint of 2.5 min for StxB-S2 and 10 min for Ctx was found to be significantly increased compared to the control. As the level of endogenous Syk in HeLa cells is low, Syk activation was investigated using transient transfection. However, activation of endogenous Syk by StxB-S2 and Ctx at 10 min was confirmed also by immunoprecipitation of pSyk (supplementary Fig. S2a). Although ricin also showed a tendency toward increased pSyk at 10 min, this was not found to be significant (supplementary Fig. S2b). No activation of Syk was seen at later time points either (supplementary Fig. S2c), which is in agreement with the inability of this toxin to induce dissociation.

As Piceatannol has been reported to affect additional signaling pathways unrelated to Syk [35], we wanted to confirm that Syk activity is involved in the dissociation process by using two unrelated Syk inhibitors. Both Syk inhibitor V and R406 are claimed to be more specific for Syk, and R406 or its prodrug R788 has entered clinical trials against rheumatoid arthritis [36]. And indeed, pre-

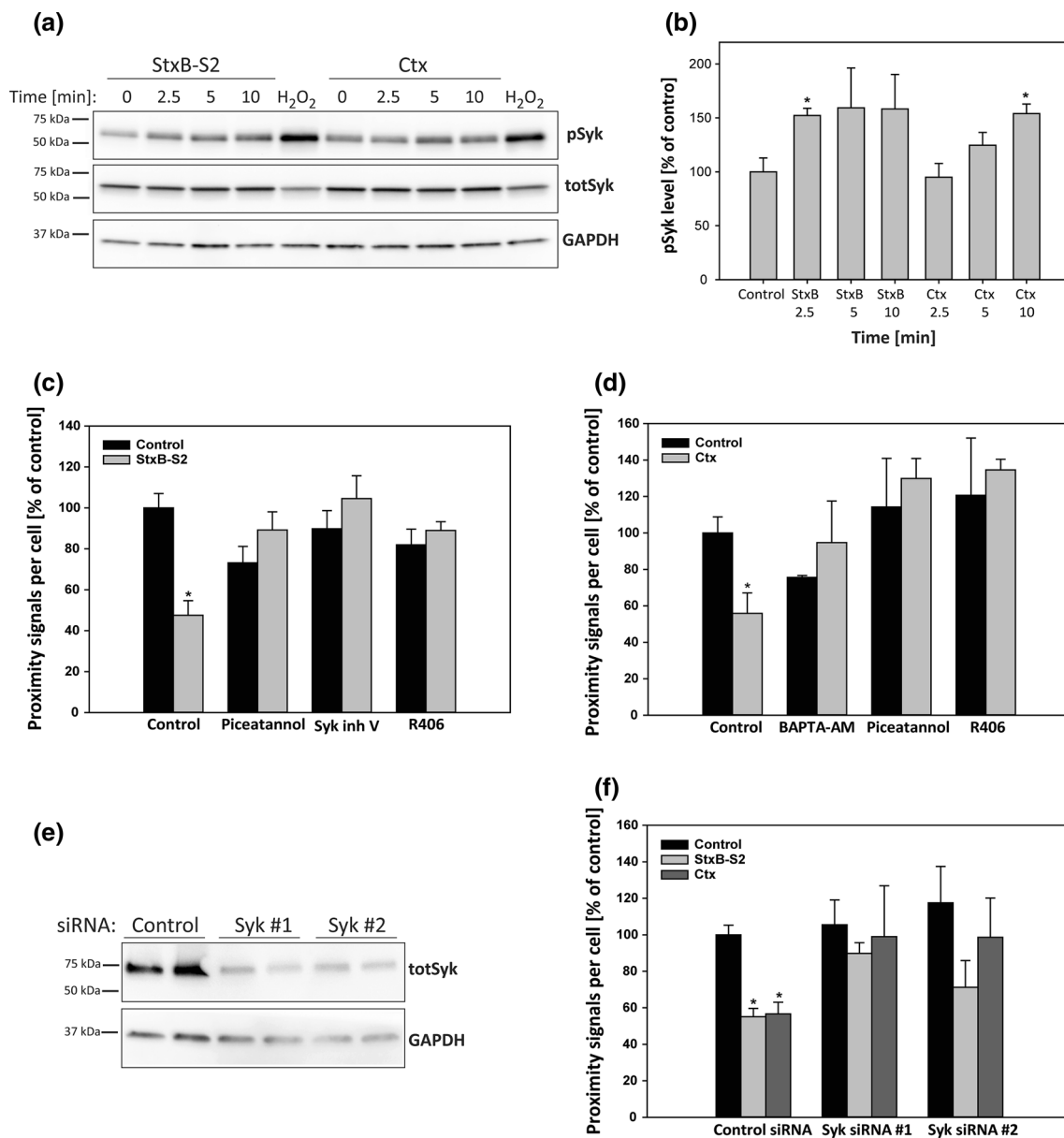


Fig. 3 Syk activation is required for the induced dissociation of cPLA₂α–AnxA1. **a** HeLa cells were transfected with a Syk-expressing plasmid for 24 h before being treated with 1 μg/ml ShigaB-sulf2 (StxB-S2) or cholera toxin (Ctx) for the indicated times, or 1 μM H₂O₂ for 10 min, and the protein lysates were subjected to immunoblot analysis using antibodies against phosphorylated Syk (pSyk), total Syk (totSyk) and GAPDH. **b** Quantification of immunoblots as shown in **a**, with pSyk levels normalized to GAPDH and presented as % of control (*n* = 4 independent experiments, mean values +SEM, **p* < 0.05). HeLa cells were pretreated with the indicated inhibitors for 30 min and treated with either 1 μg/ml StxB-S2 (**c**) or Ctx (**d**) for 10 min before being fixed, permeabilized and

subjected to PLA using cPLA₂α and AnxA1 antibodies. Images were taken by an LSM780 confocal microscope, and the number of signals per cell was quantified and presented as % of control. The mean values of at least three independent experiments are shown as +SEM, **p* < 0.05. **e** HeLa cells stably expressing GFP-Syk were transfected with either control siRNA or Syk-specific siRNAs, and after 3 days the protein lysates were subjected to immunoblot analysis using antibodies against Syk and GAPDH. **f** HeLa cells transfected as described in **e** were treated with 1 μg/ml StxB-S2 or Ctx for 10 min before being fixed, permeabilized and subjected to PLA as described in **c**, **d** (*n* = 3 independent experiments, mean values +SEM, **p* < 0.05)

treatment of HeLa cells with these inhibitors prevented the Stx-induced dissociation of the cPLA₂α–AnxA1 complex (Fig. 3c), confirming the involvement of Syk activation in the dissociation process. In line with the Stx data, Ctx-induced dissociation of the complex was also inhibited by

the Syk inhibitors Piceatannol and R406, and the calcium chelator BAPTA-AM (Fig. 3d). Furthermore, depletion of Syk using two different siRNA oligoes (Fig. 3e) also prevented the toxin-induced dissociation (Fig. 3f). From these experiments we can conclude that both Stx- and Ctx-

induced dissociation of the cPLA₂α–AnxA1 complex is dependent on intracellular calcium and Syk activation.

Shiga toxin and cholera toxin induce a rise in intracellular calcium which is required for Syk activation

Both cPLA₂α and AnxA1 are Ca²⁺-binding proteins, and it has been reported that the inhibiting effect of AnxA1 on cPLA₂α activity is dependent on the Ca²⁺ concentration, at least in vitro [37]. The inhibition is reduced as calcium is increased, in agreement with the idea that complex formation reduces cPLA₂α activity [37]. It has previously been shown that Stx1 and Stx1B induce a rapid increase in intracellular Ca²⁺ in HUVEC cells [38], and it was reported several decades ago that CtxB-binding to GM1 elevates intracellular Ca²⁺ in human Jurkat T cells [39, 40]. We therefore set out to investigate if StxB-S2 and Ctx induce changes in intracellular calcium levels in HeLa cells, and to this end, we used the calcium sensitive fluorophore Fluo-4. After loading cells with the dye, we used an automatic dispenser and plate reader to measure changes in fluorescence over time after addition of StxB-S2, Ctx or ricin. Indeed, both Stx and Ctx gave rise to an almost instant increase in intracellular calcium, which was maintained throughout the measurement period of 10 min (Fig. 4a). In contrast, ricin induced a much lower increase in calcium (Fig. 4a), which together with the lack of Syk activation (supplementary Fig. S2b-c) might explain why this toxin does not induce dissociation of the complex. The increase in intracellular calcium induced by the toxins was from extracellular sources, as no increase in calcium was seen when the assay was performed in calcium-free buffer (Fig. 4b). Thapsigargin (TG) was used as a positive control to demonstrate detection of increased cytosolic calcium from non-extracellular sources. The increase in calcium induced by TG, which was at a similar level as seen for ricin (Fig. 4a), was not sufficient to induce dissociation of the complex (supplementary Fig. S1e). Furthermore, the toxins did not induce dissociation of the cPLA₂α–AnxA1 complex in the absence of extracellular calcium (Fig. 4c), demonstrating that an influx of calcium is required for the toxin-induced dissociation.

In order to investigate if Syk activation is required for the observed increase in intracellular calcium, we performed the calcium assay after pre-treating the cells with the Syk inhibitor R406 (Fig. 4d). As expected, the increase in calcium induced by StxB-S2 (left panel) and Ctx (right panel) was inhibited by the calcium chelator BAPTA-AM. However, the Syk inhibitor R406 did not affect the increased calcium levels, demonstrating that Syk activation is not required for the observed increase in cytosolic calcium. On the other hand, increased intracellular Ca²⁺

concentration is required for Syk activation, as BAPTA-AM also inhibited the activation of Syk induced by StxB-S2 and Ctx (Fig. 4e). In line with this, we find that the calcium ionophore A23187, which in itself induces dissociation of the complex by approximately 40 % (supplementary Fig. S1c) and gives a rapid increase in intracellular calcium (supplementary Fig. S2d), leads to a rapid activation of Syk (supplementary Fig. S2e). We therefore suggest that the induced increase in intracellular calcium leads to activation of Syk, resulting in the dissociation of the cPLA₂α–AnxA1 complex.

It is not known how Stx and Ctx mediate an increase in intracellular calcium. The calcium increase was established to be from extracellular sources (Fig. 4b), so one possibility is that calcium channels in the plasma membrane are activated upon cross-linking of GSLs by the toxins, resulting in an influx of calcium into the cells. We therefore performed the calcium assay in the presence of Verapamil, an inhibitor of L-type voltage gated calcium channels, and previously shown to interfere with Stx toxicity [41]. Pre-treatment with Verapamil almost completely abolished the calcium increase induced by both StxB-S2 and Ctx (Fig. 5a). These data suggest that StxB-S2 and Ctx activate L-type voltage gated calcium channels in the plasma membrane, resulting in an influx of calcium into the cells. In line with the BAPTA-AM data (Fig. 4e), the inhibition of calcium influx prevents the activation of Syk induced by the toxins, as no activation is seen in the presence of Verapamil (Fig. 5b). L-type voltage gated calcium channels are probably not the only calcium channels involved, as also inhibition of T-type voltage gated calcium channels inhibited the toxin-induced increase in calcium to some extent (supplementary Fig. S3a).

AnxA1 translocates to late endosomes/lysosomes after dissociation

It is known that the affinity of AnxA1 for cellular membranes is dependent on the intracellular calcium concentration [13], and it has also been shown that changes in intracellular calcium can lead to translocation of cPLA₂α to intracellular membranes [16]. Thus, it was of interest to see whether the toxin-induced elevation of cytosolic Ca²⁺ would increase the fraction of AnxA1 and cPLA₂α that localizes to intracellular membranes. To this end, we performed biochemical fractionation, and indeed, there was an increase in both AnxA1 and cPLA₂α in the membrane fraction after treatment with StxB-S2 (Fig. 6a), although the increase in cPLA₂α did not reach statistical significance (Fig. 6b). Translocation in response to the calcium ionophore A23187 was used as a positive control, and Hsp90 and flotillin-2 were used as markers for the cytosolic and membrane fraction, respectively. In order to investigate to

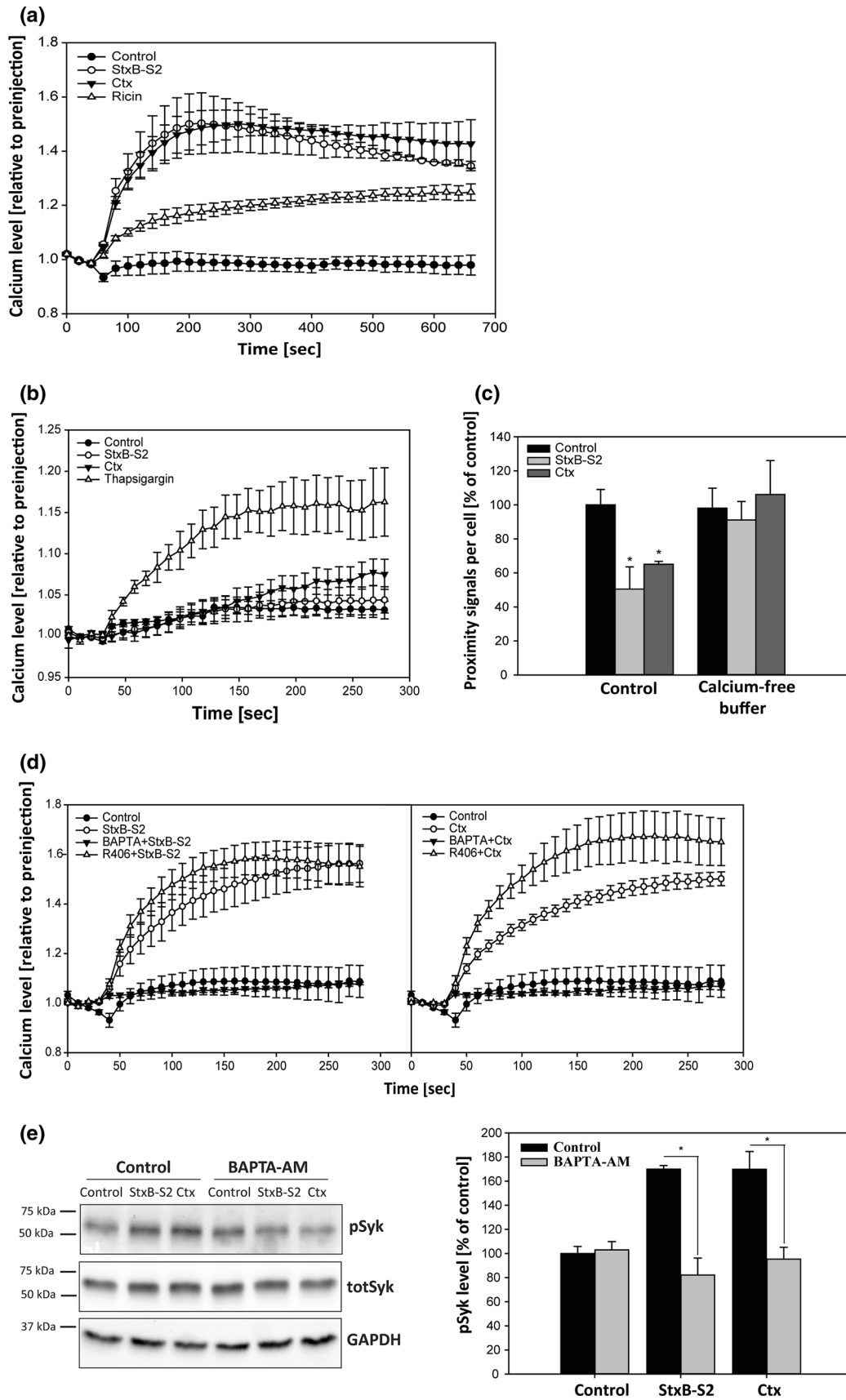


Fig. 4 Shiga toxin and cholera toxin induce an increase in intracellular calcium, which is required for Syk activation. **a** HeLa cells were loaded with cell-permeable Fluo-4 for 30 min, followed by addition of 1 $\mu\text{g/ml}$ ShigaB-sulf2 (StxB-S2), ricin or cholera toxin (Ctx). The fluorescence intensity was measured every 20 s for 10 min, and the data are normalized to the level of fluorescence prior to addition of the toxin. The mean values of at least three independent experiments are shown \pm SEM. **b** The same experiment as in **a**, but performed in calcium-free buffer. In addition to StxB-S2 and Ctx, 1.5 μM thapsigargin (TG) was added. The fluorescence intensity was measured every 10 s for 4 min and the data are normalized to the level of fluorescence prior to addition of the toxin or TG ($n = 3$ independent experiments \pm SEM). **c** HeLa cells were washed with Hepes-buffered medium (control) or calcium-free buffer before addition of 1 $\mu\text{g/ml}$ StxB-S2 or Ctx, also in the indicated buffers, for 10 min. The cells were then fixed, permeabilized and subjected to PLA using cPLA₂ α and AnxA1 antibodies. Images were taken by an LSM780 confocal microscope, and the number of signals per cell was quantified and presented as % of control ($n = 4$ independent experiments, mean values \pm SEM, $*p < 0.05$). **d** Same as in **a**, but the cells were pre-treated with the indicated inhibitors for 30 min before addition of either 1 $\mu\text{g/ml}$ StxB-S2 (*left*) or Ctx (*right*) and the fluorescence intensity was measured every 10 s for 4 min. The mean values of at least three independent experiments are shown \pm SEM. **e** HeLa cells were transfected with a Syk-expressing plasmid for 24 h before being treated with 10 μM BAPTA-AM for 30 min followed by incubation with 1 $\mu\text{g/ml}$ StxB-S2 or Ctx for 10 min. The protein lysates were subjected to immunoblot analysis using antibodies against phosphorylated Syk (pSyk), total Syk (totSyk) and GAPDH. Bar graphs show quantification of immunoblots with pSyk levels normalized to GAPDH and presented as % of control ($n = 4$ independent experiments, mean values \pm SEM, $*p < 0.05$)

which cellular membrane AnxA1 is translocated, we performed immunofluorescence analysis of AnxA1 and various intracellular markers after treatment with StxB-S2. For these experiments we used the endothelial cell line HMEC-1, and it was confirmed that StxB-S2 and Gb3 antibody induce dissociation of the cPLA₂ α -AnxA1 complex also in these cells (supplementary Fig. S1a). In line with the data from HeLa cells, the dissociation was inhibited by Piceatannol and BAPTA-AM (supplementary Fig. S1a). The immunofluorescence analysis demonstrated that treatment with StxB-S2 increased the localization of AnxA1 to LAMP1-positive late endosomes/lysosomes (Fig. 6c, d), with an increase in the Mander's colocalization coefficient from 0.12 ± 0.03 to 0.20 ± 0.05 , suggesting that AnxA1 partly translocates to late endosomes/lysosomes after dissociation.

Discussion

In this study we have investigated the mechanisms by which cross-linking of GSLs at the plasma membrane induce dissociation of a cytosolic complex with reported functions in membrane traffic. The data presented provide new insight into how ligand binding to GSLs at the outer

leaflet of the plasma membrane may have consequences for intracellular signaling and transport.

As described in the introduction, GSLs are enriched in membrane domains termed lipid rafts [3]. It has been suggested that to function as signaling platforms, lipid rafts have to cluster into larger domains that can engage and recruit signaling complexes [42]. In agreement with this, our data strongly indicate that multivalent binding of GSLs is required to induce the intracellular events described in this study. We therefore suggest that cross-linking of GSLs at the plasma membrane impose changes to the membrane domain/lipid raft, which facilitates calcium-transport into the cytosol and activation of Syk. There seems to be an involvement of lipid rafts in this process, as extraction of cholesterol by mCD inhibits the ability of StxB-S2 and Ctx to induce dissociation of the complex. Interestingly, StxB has been demonstrated to be capable of forming a new membrane phase characterized by lipid compaction [43]. It was proposed that StxB-binding to Gb3 generates toxin clusters at the plasma membrane, and that more Gb3 molecules are recruited underneath these clusters resulting in membrane thickening and lipid packing [43]. Cross-linking of GM1 induced by CtxB (the binding subunit of Ctx) has also been shown to occur in cells and to trigger phase separation in model membranes [44]. Although the data presented here indicate that Stx and Ctx induce complex dissociation via a similar mechanism, one cannot exclude toxin-specific properties that could result in different dissociation kinetics for the cPLA₂ α -AnxA1 complex. It has for instance been shown that StxB bound to Gb3 is much more mobile in the membrane than GM1-bound CtxB, and that actin plays an important role in constraining the diffusion of CtxB [45]. The cross-linking ability of the two toxins may also be different, as each StxB subunit has three binding sites for Gb3 [22], whereas each CtxB subunit has only one binding site for GM1 [46]. These are issues that should be explored in future studies.

How the toxins are able to induce an influx of calcium into the cells has until now been unknown. From our data it is clear that the increase in intracellular calcium is from extracellular sources. It has been described that key proteins involved in Ca²⁺ signaling are localized in discrete membrane domains/lipid rafts, and that the clustering of Ca²⁺ channels and their regulators in these micro-domains provide an exquisite way of regulating Ca²⁺-mediated cellular functions in time and space (for review, see [47]). As discussed above, small membrane domains might arise from the toxin-induced cross-linking of their GSL receptors, and specific Ca²⁺ channels could then be recruited to and activated in such domains. In support of this, we find that Verapamil, an inhibitor of L-type voltage gated calcium channels, drastically reduces the influx of calcium induced by StxB-S2 and Ctx. Verapamil did not completely

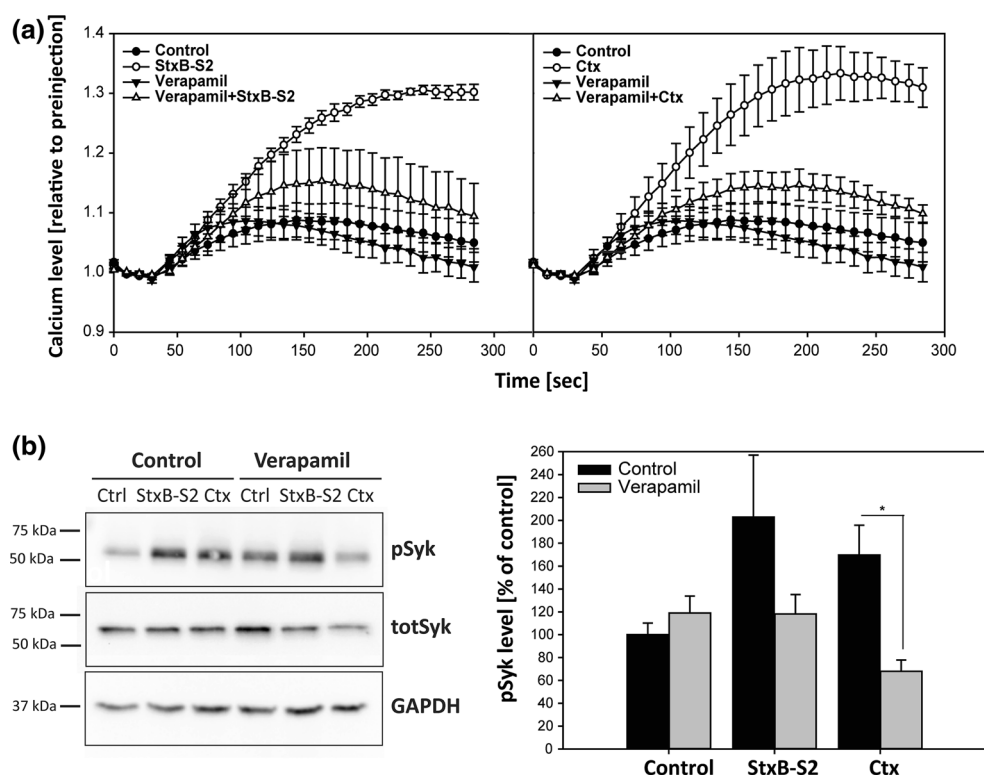


Fig. 5 Verapamil inhibits the increase in intracellular calcium and Syk activation induced by Shiga and cholera toxin. **a** HeLa cells were loaded with cell-permeable Fluo-4 for 30 min in the absence or presence of 250 μ M verapamil, followed by the addition of 1 μ g/ml ShigaB-sulf2 (StxB-S2) or cholera toxin (Ctx). The fluorescence intensity was measured every 10 s for 4 min, and the data are normalized to the level of fluorescence prior to addition of the toxins. The mean values of at least three independent experiments are

shown \pm SEM. **b** HeLa cells were transfected with an Syk-expressing plasmid for 24 h before being treated with 250 μ M verapamil for 30 min followed by incubation with 1 μ g/ml StxB-S2 or Ctx for 10 min. The protein lysates were subjected to immunoblot analysis using antibodies against phosphorylated Syk (pSyk), total Syk (totSyk) and GAPDH. Bar graphs show quantification of immunoblots with pSyk levels normalized to GAPDH and presented as % of control ($n = 3$ independent experiments, mean values \pm SEM, * $p < 0.05$)

abolish the increase in calcium induced by the toxins, so there might be additional factors involved. Activation of other types of calcium channels could of course also contribute, and we did indeed see some reduction in the toxin-induced calcium influx also by inhibiting T-type calcium channels by the use of ML218. Alternatively, cross-linking of GSLs might impose structural changes to the plasma membrane which could alter the general calcium permeability of the membrane. However, as Verapamil inhibited the calcium influx induced by StxB-S2 and Ctx by 80 % and 87 %, respectively, the contribution from changes in the general calcium permeability of the membrane would only play a minor role.

The involvement of calcium in the dissociation process was deduced from the ability of the calcium chelator BAPTA-AM and the calcium ionophore A23187 to inhibit the Stx-induced dissociation of the cPLA₂ α -AnxA1 complex. Of note, A23187 alone induced complex dissociation by approximately 40 %. A23187 gives rise to an instant increase in intracellular calcium of the cells, as well as a rapid activation of Syk, which would explain why A23187

induces complex dissociation without GSL cross-linking. Why there is a modest effect of BAPTA-AM on the complex is not clear, as it obviously does not induce increases in intracellular calcium and it also does not activate Syk. It could suggest that stable complex formation requires a certain minimal level of calcium, which is not available in the presence of BAPTA-AM.

Shiga toxin has been shown to induce plasma membrane invaginations involved in its uptake into cells [48–52]. In a recent paper, Renard and coworkers [48] demonstrate that endophilin A2 is recruited to sites of StxB (and CtxB) internalization, functioning in membrane scission. Work by Boucrot et al. [53] published simultaneously, characterize this endophilin A2-dependent and clathrin-independent endocytic process and named it FEME (fast endophilin-mediated endocytosis). To investigate whether such Stx-induced membrane invaginations and FEME are required for the signaling here studied, we tested the possible involvement of phosphoinositide 3-kinase (PI(3)K), as FEME was shown to be dependent on, among many other factors, PI(3)K activity [53]. However, the Stx-induced

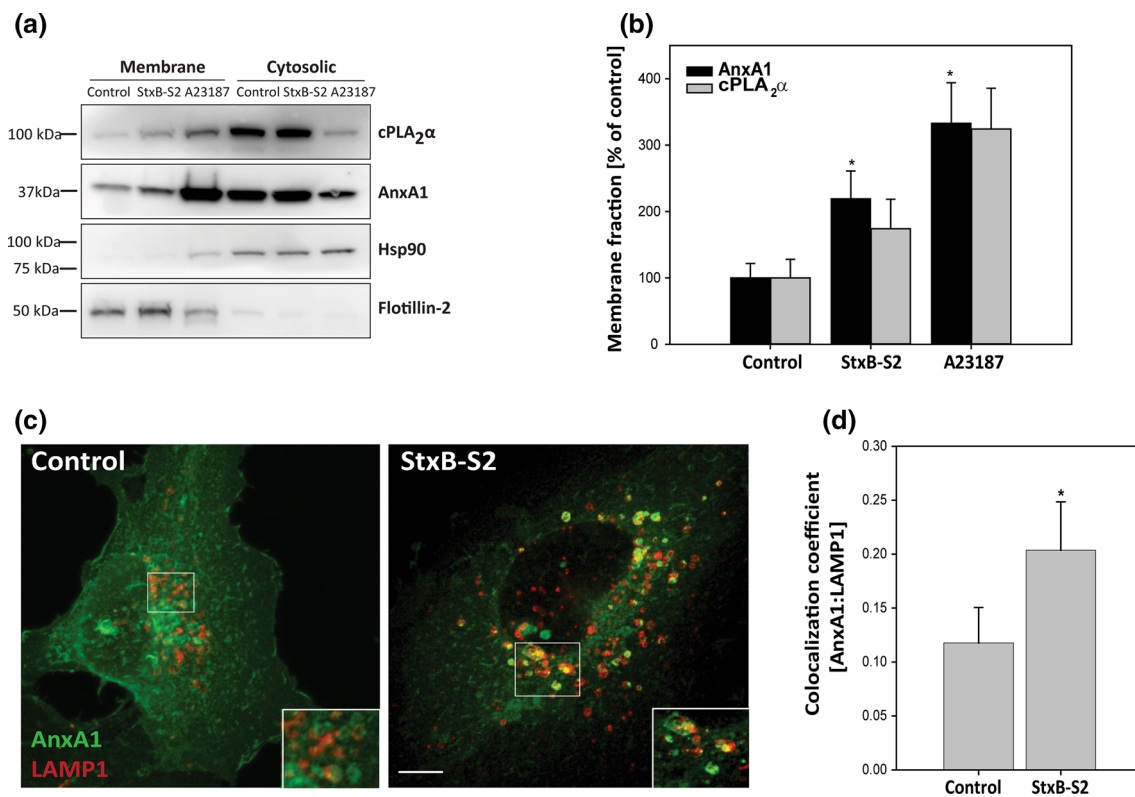


Fig. 6 ShigaB-sulf2 induces translocation of AnxA1 to intracellular membranes. **a** HeLa cells were treated with 1 μ g/ml ShigaB-sulf2 (StxB-S2) or 2 μ M A23187 for 30 min, before the protein lysates were separated into cytosolic and membrane fractions and subjected to immunoblot analysis with antibodies as indicated. **b** Quantification of membrane fractions with AnxA1 and cPLA₂α levels normalized to flotillin-2 and presented as % of control. The mean values of at least three independent experiments are shown as +SEM, * $p < 0.05$. **c** HMEC-1 cells were treated with 1 μ g/ml StxB-S2 for 30 min before

being fixed, permeabilized and subjected to immunofluorescence analysis using AnxA1 and LAMP1 antibodies. Images were acquired with an LSM780 confocal microscope, and the maximum intensity projection of 16 sections is shown. *Scale bar*, 5 μ m. **d** Confocal images (single sections) obtained in experiments as described in **c** were analyzed, and the Manders colocalization coefficient between AnxA1 and LAMP1 was determined ($n = 4$ independent experiments, mean values +SEM, * $p < 0.05$)

dissociation of the cPLA₂α–AnxA1 complex described in our study did not depend on PI(3)K activity, as neither wortmannin or LY294002 or Akt Inhibitor VIII (data not shown) interfered with the ability of the toxin to induce dissociation. Furthermore, inhibition of actin polymerization also interfered with the FEME pathway [53], however, treatment with Latrunculin B did not affect the calcium influx induced by Stx and Ctx in our study. Additionally, complex dissociation was clearly induced by an IgM anti-Gb3 antibody even though an IgM anti-Gb3 antibody did not induce membrane invaginations in Gb3-containing GUVs [49]. Together these data suggests that Stx-induced invaginations and the FEME pathway are most likely not involved in the observed dissociation of the cPLA₂α–AnxA1 complex.

It has recently been described that Gal3 is a driver of the biogenesis of endocytic carriers called CLIC (clathrin-independent carriers) and that this process is dependent on the presence of GSLs [54]. Here, it was suggested that membrane-bound Gal3 oligomerizes and binds GSLs,

thereby inducing endocytic invaginations [54]. One could imagine that Gal3-oligomer binding of GSLs would result in GSL cross-linking and potentially induce cPLA₂α–AnxA1 complex dissociation. However, our data clearly show that Gal3 does not induce dissociation of the complex. This could either mean that although we demonstrate that Gal3 binds to the surface of HeLa cells, it is not able to bind and cross-link GSLs in our system, or that the binding/cross-linking is not sufficient to induce the intracellular signaling leading to dissociation. In support of this, we did not observe any Syk activation upon Gal3 treatment (data not shown).

It has previously been shown that AnxA1 has an inhibiting effect on cPLA₂α activity, most likely by preventing its recruitment to the phospholipid substrate [55–57]. The inhibition is reduced as calcium is increased, in agreement with the idea that complex formation reduces cPLA₂α activity [37]. Complex dissociation is therefore correlated with increased cPLA₂α activity, which again would affect the membrane structure and function [58]. It

has been shown that increased intracellular Ca^{2+} promotes translocation of cPLA₂α to intracellular membranes, preferentially to the Golgi apparatus, but also to other intracellular membranes depending on the Ca^{2+} concentration [16–18]. In line with this, our data suggest that cPLA₂α is partly translocated to membranes after StxB-S2 treatment. However, we were unable to identify the nature of these membranes as we could not detect any significant changes in the localization of cPLA₂α by immunofluorescence analysis, by staining for endogenous cPLA₂α or by overexpression of cPLA₂α-GFP (data not shown). This might indicate that the toxin-induced increase in Ca^{2+} is not sufficient to induce a stable and detectable change in localization of cPLA₂α. One might speculate that if cPLA₂α indeed is translocated at least partly to the Golgi apparatus in response to the toxin-induced Ca^{2+} influx, cPLA₂α could be involved in toxin transport to and through the Golgi, as we have previously found that inhibition of cPLA₂ reduces Stx transport to the Golgi [12]. The fractionation data also show that AnxA1 is translocated to membranes upon StxB-S2 treatment, and the immunofluorescence data suggest that these membranes are at least partly late endosomal/lysosomal membranes as an increase in colocalization with LAMP1 was seen. We analyzed the colocalization of AnxA1 with several other intracellular markers as well, but did not observe any change in colocalization with the early endosomal marker EEA1, the late endosomal marker Rab7 or the recycling endosomal marker Rab11 after treatment with StxB-S2 (data not shown). In a study by Rescher et al. [59], Ca^{2+} binding resulted in AnxA1 localization to early endosomal membranes, while in our experiments we find increased colocalization with the late endosomal/lysosomal marker LAMP1. This apparent discrepancy might be due to the fact that our experiments were performed on cells stained for endogenous AnxA1, whereas the work by Rescher et al. was performed in HeLa cells overexpressing GFP-tagged AnxA1. It could also reflect differences in intracellular calcium concentrations between the studies, which would affect the membrane affinity of AnxA1. Further work is required to explore in more detail to which membranes the complex components are translocated upon GSL cross-linking.

In summary, we propose that GSL cross-linking at the plasma membrane promotes the generation of membrane microdomains, induction of a calcium influx and activation of Syk. These events then lead to dissociation of the cPLA₂α–AnxA1 complex, followed by translocation to intracellular membranes, where these factors are reported to play a role in membrane trafficking events. The data reveal a novel mechanism for transfer of signals from interactions at the outer leaflet of the plasma membrane to intracellular events involved in membrane transport.

Acknowledgments We thank Anne Engen for excellent assistance with cell culturing, Anne-Mari Gjestvang Pedersen and Roger Simm for purification of Shiga toxins, and Maria Lyngaas Torgersen and Sascha Pust for critically reading the manuscript. This work was supported by grants from the South-Eastern Norway Regional Health Authority, the Norwegian Cancer Society and the Norwegian Research Council through its Centres of Excellence funding scheme, project number 179571.

References

1. van Meer G, Voelker DR, Feigenson GW (2008) Membrane lipids: where they are and how they behave. *Nat Rev Mol Cell Biol* 9:112–124
2. D'Angelo G, Capasso S, Sticco L, Russo D (2013) Glycosphingolipids: synthesis and functions. *FEBS J* 280:6338–6353
3. Simons K, Sampaio JL (2011) Membrane organization and lipid rafts. *Cold Spring Harb Perspect Biol* 3:a004697
4. Suzuki KG (2012) Lipid rafts generate digital-like signal transduction in cell plasma membranes. *Biotechnol J* 7:753–761
5. Furukawa K, Tokuda N, Okuda T, Tajima O, Furukawa K (2004) Glycosphingolipids in engineered mice: insights into function. *Semin Cell Dev Biol* 15:389–396
6. Proia RL (2003) Glycosphingolipid functions: insights from engineered mouse models. *Philos Trans R Soc Lond B Biol Sci* 358:879–883
7. Engedal N, Skotland T, Torgersen ML, Sandvig K (2011) Shiga toxin and its use in targeted cancer therapy and imaging. *Microb Biotechnol* 4:32–46
8. Hakomori S, Zhang Y (1997) Glycosphingolipid antigens and cancer therapy. *Chem Biol* 4:97–104
9. Kolter T (2011) A view on sphingolipids and disease. *Chem Phys Lipids* 164:590–606
10. Bergan J, Dyve Lingelem AB, Simm R, Skotland T, Sandvig K (2012) Shiga toxins. *Toxicon* 60:1085–1107
11. Sandvig K, Bergan J, Kavaliauskiene S, Skotland T (2014) Lipid requirements for entry of protein toxins into cells. *Prog Lipid Res* 54:1–13
12. Tcatchoff L, Andersson S, Utskarpen A, Klokk TI, Skanland SS, Pust S, Gerke V, Sandvig K (2012) Annexin A1 and A2: roles in retrograde trafficking of Shiga toxin. *PLoS One* 7:e40429
13. Gerke V, Creutz CE, Moss SE (2005) Annexins: linking Ca^{2+} signalling to membrane dynamics. *Nat Rev Mol Cell Biol* 6:449–461
14. Burke JE, Dennis EA (2009) Phospholipase A2 structure/function, mechanism, and signaling. *J Lipid Res* 50(Suppl):S237–S242
15. San Pietro E, Capestrano M, Polishchuk EV, DiPentima A, Trucco A, Zizza P, Mariggio S, Pulvirenti T, Sallèse M, Tete S, Mironov AA, Leslie CC, Corda D, Luini A, Polishchuk RS (2009) Group IV phospholipase A(2)α controls the formation of inter-cisternal continuities involved in intra-Golgi transport. *PLoS Biol* 7:e1000194
16. Evans JH, Spencer DM, Zweifach A, Leslie CC (2001) Intracellular calcium signals regulating cytosolic phospholipase A2 translocation to internal membranes. *J Biol Chem* 276:30150–30160
17. Evans JH, Leslie CC (2004) The cytosolic phospholipase A2 catalytic domain modulates association and residence time at Golgi membranes. *J Biol Chem* 279:6005–6016
18. Grewal S, Ponnambalam S, Walker JH (2003) Association of cPLA₂α and COX-1 with the Golgi apparatus of A549 human lung epithelial cells. *J Cell Sci* 116:2303–2310

19. Lauvrak SU, Walchli S, Iversen TG, Slagsvold HH, Torgersen ML, Spilsberg B, Sandvig K (2006) Shiga toxin regulates its entry in a Syk-dependent manner. *Mol Biol Cell* 17:1096–1109
20. Kvalvaag AS, Pust S, Sundet KI, Engedal N, Simm R, Sandvig K (2013) The ERM proteins ezrin and moesin regulate retrograde Shiga toxin transport. *Traffic* 14:839–852
21. Rapak A, Falnes PO, Olsnes S (1997) Retrograde transport of mutant ricin to the endoplasmic reticulum with subsequent translocation to cytosol. *Proc Natl Acad Sci U S A* 94:3783–3788
22. Lingwood CA, Law H, Richardson S, Petric M, Brunton JL, De GS, Karmali M (1987) Glycolipid binding of purified and recombinant *Escherichia coli* produced verotoxin in vitro. *J Biol Chem* 262:8834–8839
23. Sandvig K, Torgersen ML, Engedal N, Skotland T, Iversen TG (2010) Protein toxins from plants and bacteria: probes for intracellular transport and tools in medicine. *FEBS Lett* 584:2626–2634
24. Wernick NL, Chinnapen DJ, Cho JA, Lencer WI (2010) Cholera toxin: an intracellular journey into the cytosol by way of the endoplasmic reticulum. *Toxins (Basel)* 2:310–325
25. Ahmad N, Gabius HJ, Andre S, Kaltner H, Sabesan S, Roy R, Liu B, Macaluso F, Brewer CF (2004) Galectin-3 precipitates as a pentamer with synthetic multivalent carbohydrates and forms heterogeneous cross-linked complexes. *J Biol Chem* 279:10841–10847
26. Lepur A, Salomonsson E, Nilsson UJ, Leffler H (2012) Ligand induced galectin-3 protein self-association. *J Biol Chem* 287:21751–21756
27. Collins PM, Bum-Erdene K, Yu X, Blanchard H (2014) Galectin-3 interactions with glycosphingolipids. *J Mol Biol* 426:1439–1451
28. Katagiri YU, Mori T, Nakajima H, Katagiri C, Taguchi T, Takeda T, Kiyokawa N, Fujimoto J (1999) Activation of Src family kinase yes induced by Shiga toxin binding to globotriaosyl ceramide (Gb3/CD77) in low density, detergent-insoluble microdomains. *J Biol Chem* 274:35278–35282
29. Mori T, Kiyokawa N, Katagiri YU, Taguchi T, Suzuki T, Sekino T, Sato N, Ohmi K, Nakajima H, Takeda T, Fujimoto J (2000) Globotriaosyl ceramide (CD77/Gb3) in the glycolipid-enriched membrane domain participates in B-cell receptor-mediated apoptosis by regulating lyn kinase activity in human B cells. *Exp Hematol* 28:1260–1268
30. Walchli S, Skånland SS, Gregers TF, Lauvrak SU, Torgersen ML, Ying M, Kuroda S, Maturana A, Sandvig K (2008) The Mitogen-activated protein kinase p38 links Shiga Toxin-dependent signaling and trafficking. *Mol Biol Cell* 19:95–104
31. Torgersen ML, Walchli S, Grimmer S, Skånland SS, Sandvig K (2007) Protein kinase C δ is activated by Shiga toxin and regulates its transport. *J Biol Chem* 282:16317–16328
32. Utskarpen A, Massol R, van DB, Lauvrak SU, Kirchhausen T, Sandvig K (2010) Shiga toxin increases formation of clathrin-coated pits through Syk kinase. *PLoS One* 5:e10944
33. Walchli S, Aasheim HC, Skånland SS, Spilsberg B, Torgersen ML, Rosendal KR, Sandvig K (2009) Characterization of clathrin and Syk interaction upon Shiga toxin binding. *Cell Signal* 21:1161–1168
34. Mocsai A, Ruland J, Tybulewicz VL (2010) The SYK tyrosine kinase: a crucial player in diverse biological functions. *Nat Rev Immunol* 10:387–402
35. Piotrowska H, Kucinska M, Murias M (2012) Biological activity of piceatannol: leaving the shadow of resveratrol. *Mutat Res* 750:60–82
36. Nijjar JS, Tindell A, McInnes IB, Siebert S (2013) Inhibition of spleen tyrosine kinase in the treatment of rheumatoid arthritis. *Rheumatology (Oxford)* 52:1556–1562
37. Kim KM, Kim DK, Park YM, Kim CK, Na DS (1994) Annexin-I inhibits phospholipase A2 by specific interaction, not by substrate depletion. *FEBS Lett* 343:251–255
38. Liu F, Huang J, Sadler JE (2011) Shiga toxin (Stx)1B and Stx2B induce von Willebrand factor secretion from human umbilical vein endothelial cells through different signaling pathways. *Blood* 118:3392–3398
39. Dixon SJ, Stewart D, Grinstein S, Spiegel S (1987) Transmembrane signaling by the B subunit of cholera toxin: increased cytoplasmic free calcium in rat lymphocytes. *J Cell Biol* 105:1153–1161
40. Gouy H, Deterre P, Debre P, Bismuth G (1994) Cell calcium signaling via GM1 cell surface gangliosides in the human Jurkat T cell line. *J Immunol* 152:3271–3281
41. Sandvig K, Brown JE (1987) Ionic requirements for entry of Shiga toxin from *Shigella dysenteriae* 1 into cells. *Infect Immun* 55:298–303
42. Rajendran L, Simons K (2005) Lipid rafts and membrane dynamics. *J Cell Sci* 118:1099–1102
43. Windschiegel B, Orth A, Romer W, Berland L, Stechmann B, Bassereau P, Johannes L, Steinem C (2009) Lipid reorganization induced by Shiga toxin clustering on planar membranes. *PLoS One* 4:e6238
44. Hammond AT, Heberle FA, Baumgart T, Holowka D, Baird B, Feigenson GW (2005) Crosslinking a lipid raft component triggers liquid ordered-liquid disordered phase separation in model plasma membranes. *Proc Natl Acad Sci USA* 102:6320–6325
45. Day CA, Kenworthy AK (2012) Mechanisms underlying the confined diffusion of cholera toxin B-subunit in intact cell membranes. *PLoS One* 7:e34923
46. Merritt EA, Sarfaty S, Van den Akker F, L'Hoir C, Martial JA, Hol WG (1994) Crystal structure of cholera toxin B-pentamer bound to receptor GM1 pentasaccharide. *Protein Sci* 3:166–175
47. Pani B, Singh BB (2009) Lipid rafts/caveolae as microdomains of calcium signaling. *Cell Calcium* 45:625–633
48. Renard HF, Simunovic M, Lemiere J, Boucrot E, Garcia-Castillo MD, Arumugam S, Chambon V, Lamaze C, Wunder C, Kenworthy AK, Schmidt AA, McMahon HT, Sykes C, Bassereau P, Johannes L (2015) Endophilin-A2 functions in membrane scission in clathrin-independent endocytosis. *Nature* 517:493–496
49. Romer W, Berland L, Chambon V, Gaus K, Windschiegel B, Tenza D, Aly MR, Fraissier V, Florent JC, Perrais D, Lamaze C, Raposo G, Steinem C, Sens P, Bassereau P, Johannes L (2007) Shiga toxin induces tubular membrane invaginations for its uptake into cells. *Nature* 450:670–675
50. Romer W, Pontani LL, Sorre B, Rentero C, Berland L, Chambon V, Lamaze C, Bassereau P, Sykes C, Gaus K, Johannes L (2010) Actin dynamics drive membrane reorganization and scission in clathrin-independent endocytosis. *Cell* 140:540–553
51. Rydell GE, Renard HF, Garcia-Castillo MD, Dingli F, Loew D, Lamaze C, Romer W, Johannes L (2014) Rab12 localizes to Shiga toxin-induced plasma membrane invaginations and controls toxin transport. *Traffic* 15:772–787
52. Safouane M, Berland L, Callan-Jones A, Sorre B, Romer W, Johannes L, Toombes GE, Bassereau P (2010) Lipid cosorting mediated by shiga toxin induced tubulation. *Traffic* 11:1519–1529
53. Boucrot E, Ferreira AP, Almeida-Souza L, Debard S, Vallis Y, Howard G, Bertot L, Sauvonnnet N, McMahon HT (2015) Endophilin marks and controls a clathrin-independent endocytic pathway. *Nature* 517:460–465
54. Lakshminarayan R, Wunder C, Becken U, Howes MT, Benzing C, Arumugam S, Sales S, Ariotti N, Chambon V, Lamaze C, Loew D, Shevchenko A, Gaus K, Parton RG, Johannes L (2014) Galectin-3 drives glycosphingolipid-dependent biogenesis of clathrin-independent carriers. *Nat Cell Biol* 16:595–606

55. Herbert SP, Odell AF, Ponnambalam S, Walker JH (2007) The confluence-dependent interaction of cytosolic phospholipase A2 α with annexin A1 regulates endothelial cell prostaglandin E2 generation. *J Biol Chem* 282:34468–34478
56. Kim SW, Rhee HJ, Ko J, Kim YJ, Kim HG, Yang JM, Choi EC, Na DS (2001) Inhibition of cytosolic phospholipase A2 by annexin I. Specific interaction model and mapping of the interaction site. *J Biol Chem* 276:15712–15719
57. Oh J, Rhee HJ, Kim S, Kim SB, You H, Kim JH, Na DS (2000) Annexin-I inhibits PMA-induced c-fos SRE activation by suppressing cytosolic phospholipase A2 signal. *FEBS Lett* 477:244–248
58. Brown WJ, Chambers K, Doody A (2003) Phospholipase A2 (PLA2) enzymes in membrane trafficking: mediators of membrane shape and function. *Traffic* 4:214–221
59. Rescher U, Zobiack N, Gerke V (2000) Intact Ca²⁺-binding sites are required for targeting of annexin 1 to endosomal membranes in living HeLa cells. *J Cell Sci* 113(Pt 22):3931–3938